Exploring aerosol-cloud interaction in Southeast Pacific marine stratocumulus during VOCALS regional experiment

Sudhakar, Dipu.[1,✉], **Johannes, Quaas.**[1]

[1] *Leipzig for Meteorology, Universität Leipzig, Germany*
✉*e-mail: dipu.sudhakar@uni-leipzig.de*

Summary: The marine stratocumulus clouds are highly sensitive to aerosol perturbations. In this study, we have explored the cloud susceptibility to aerosol using satellite observation and multi-model simulations over the Southeast Pacific Ocean (SEP). The climatology of satellite observation indicates that SEP is a relatively clean area with low aerosol optical depth (AOD). The SEP is a region of marine stratocumulus deck with cloud fraction (CF) reaching as high as 90% in many regions, with relatively low ($140\,cm^{-3}$) cloud droplet number concentration (CDNC) over the marine environment, and it increases as it moves towards the coast. The joint histogram analysis shows that the AOD-CDNC relation shows positive sensitivity and a non-linear CDNC-LWP (liquid water path) relationship; however, a negative sensitivity is dominant. The multi-model analysis shows that most models have a strong positive AOD-CDNC sensitivity, suggesting that the cloud albedo effect leads to net cooling. The general circulation models (GCM) reveal a negative radiative forcing (-0.28 to -1.36 $W\,m^{-2}$) at the top of the atmosphere (TOA) when using the flux method. It supports the positive AOD-CDNC sensitivity and the resulting negative radiative forcing in GCMs. However, the CDNC-LWP shows a diverse relation in the models. In the GCMs, the effect of cloud microphysics is not considered while estimating the net radiative forcing. To include the effect of cloud microphysics in the radiative forcing estimates, we have proposed a statistical approach to calculate the net radiative forcing. The results show that the net radiative forcing is sensitive to the LWP change due to the aerosol perturbation.

Zusammenfassung: Die marinen Stratocumulus-Wolken reagieren sehr empfindlich auf Aerosol-Störungen. In dieser Studie haben wir die Anfälligkeit der Wolken für Aerosol anhand von Satellitenbeobachtungen und Multi-Modellsimulationen über dem Südostpazifik (SEP) untersucht. Die Klimatologie der Satellitenbeobachtung zeigt, dass der SEP ein relativ sauberes Gebiet mit geringer Aerosol optischer Dicke (AOD) ist. Der SEP ist eine Region mit mariner Stratocumulus-Decke mit einer Wolkbedeckungsgrad (CF), der in vielen Regionen bis zu 90% erreicht, mit einer relativ niedrigen ($140\,cm^{-3}$) Wolkentröpfchenanzahlkonzentration (CDNC) über der marinen Umgebung, und sie nimmt in Richtung Küste zu. Die gemeinsame Histogramm-Analyse zeigt, dass die AOD-CDNC-Beziehung eine positive Sensitivität und eine nicht-lineare CDNC-LWP-Beziehung (Flüssigwasserpfad) aufweist; allerdings ist eine negative Sensitivität vorherrschend. Die Multi-Modellanalyse zeigt, dass die meisten Modelle eine stark positive AOD-CDNC-Empfindlichkeit aufweisen, was darauf hindeutet, dass der Wolkenalbedo-Effekt eine Nettokühlung bewirkt. Die allgemeinen Zirkulationsmodelle

(GCM) zeigen einen negativen Strahlungsantrieb (-0,28 bis -1,36 $\mathrm{W\,m^{-2}}$) am Oberrand der Atmosphäre (TOA), wenn die Flussmethode verwendet wird. Dies unterstützt die positive AOD-CDNC-Empfindlichkeit und den daraus resultierenden negativen Strahlungsantrieb in GCMs. Der CDNC-LWP zeigt jedoch unterschiedliche Abhängigkeiten in den Modellen. In den GCMs wird die Wirkung der Wolkenmikrophysik bei der Abschätzung des Netto-Strahlungsantriebs nicht berücksichtigt. Um die Auswirkungen der Wolkenmikrophysik auf den Strahlungsantrieb einzubeziehen, haben wir einen statistischen Ansatz zur Berechnung des Nettostrahlungsantriebs gewählt. Die Ergebnisse zeigen, dass der Nettostrahlungsantrieb empfindlich auf die LWP-Änderung durch die Aerosolstörung reagiert.

1 Introduction

Aerosols, clouds, and their interaction continue to be the primary contributor to the uncertainty in assessing the Earth's radiation budget estimates (Forster et al., 2021; Mülmenstädt and Feingold, 2018). Atmospheric aerosols can act as cloud condensation nuclei that modulate cloud micro and macrophysical properties (Twomey, 1977; Charlson et al., 1992). Twomey (1977) reported the relation between aerosol concentration, cloud droplet number concentration (CDNC) and cloud albedo. It hypothesized that an increased aerosol loading could modify the CDCN, which enhances the cloud albedo, commonly known as radiative forcing due to aerosol-cloud interaction (Bellouin et al., 2020; Forster et al., 2021). Further, at higher CDNC, the LWP may enhance or decrease, subjected to rapid adjustments to aerosol-cloud interactions (Albrecht, 1989). Thus, aerosols influence the cloud via modifying microphysical processes and substantially impact their radiative forcing (Menon et al., 2002). Satellite imagery has been proven that ship tracks (Goren and Rosenfeld, 2012) and smoke plumes (Goren and Rosenfeld, 2015) are evidence of aerosol-cloud interaction and subsequent radiative effect.

Quantifying the mechanisms responsible for aerosol radiative forcing and its representation in models has been proven to be challenging. Nevertheless, several studies investigated the aerosol-cloud interaction and estimated radiative forcing with a wide range of uncertainty (Twomey, 1977; Menon et al., 2008; Quaas et al., 2008; Wood et al., 2011). The uncertainty may arise from wide observational scales and platforms (McComiskey and Feingold, 2012).

In-situ observation plays a crucial role in unfolding the uncertainties in aerosol-cloud interaction. The VAMOS (Variability of the American Monsoon Systems) Ocean-Cloud-Atmosphere-Land study (VOCALS, Wood et al., 2011) is an international program designed to understand the physical and chemical processes of the coupled climate system of the Southeast Pacific (SEP). The VOCALS campaign is categorized into the VOCAL regional experiment (in-situ observations) and the VOCAL numerical model experiment. The Weather Research and Forecasting model coupled to Chemistry (WRF-chem) and COnsortium for Small-scale MOdeling - Aerosols and Reactive Trace gases (COSMO-ART) are the regional models actively participating in the VOCALS modelling experiment. They have compared the aerosol and cloud characteristics over the SEP with observation and are in good agreement (Wood et al., 2011; Wyant et al., 2015). Additionally, Min et al. (2012) reported a strong correlation between satellite observation, specifically aerosol and cloud optical properties, with the VOCALS in-situ

measurements.

This study explores the aerosol-cloud interaction over the SEP during the VOCALS experiment. For this, we have used satellite observations and multi-model simulations (both regional and global models) to explore the aerosol-cloud interaction over the SEP during the VOCALS experiment. Further, to have a better representation of radiative forcing due to the aerosol-cloud interaction, we have proposed a new statistical method to calculate radiative forcing by considering the cloud's optical properties. Detailed descriptions of numerical models, satellite data sets, and the statistical approach are given in section 2. Results of the analysis have been described in section 3, and the summary and conclusions are presented in section 4.

2 Data and methods

2.1 Regional models

In this study, we have considered simulations from the regional model, WRF-Chem (Grell et al., 2005), and COSMO-ART (Vogel et al., 2006). In both cases, the simulations were carried out for the time period of 15 October to 15 November 2008, which were run continuously in free-running mode. There are two sets of WRF-chem model simulations carried out by the University of Iowa (IOWA, Saide et al., 2012) and the Pacific Northwest National Laboratory (PNNL, Yang et al., 2012). The IOWA simulation uses the lateral boundary condition from the National Centers for Environmental Prediction (NCEP) global Final Analysis (FNL), and the PNNL uses the lateral boundary condition from the NCEP's Global Forecast System (GFS) analyses. The COSMO-ART has been configured, and simulations are carried out by the Karlsruhe Institute of Technology (KIT) research group. The COSMO-ART is based on the mesoscale model system (Vogel et al., 2006). It replaces the meteorological module with an optional weather forecast model COSMO of the Deutscher Wetterdienst (DWD). The modelling system consists of gas-phase chemistry, and aerosol dynamics are online coupled with the COSMO model. The model is initialized and forced with the reanalysis data, the global meteorological model GME (Global Model of the Earth). A detailed description of the above-mentioned regional models can be obtained from Wang et al. (2011), Wood et al. (2011), and Wyant et al. (2015).

2.2 Global models

Although several GCMs are also contributed to VOCALS Rex, we have considered the Aerosol Comparison between Observations and Models (AeroCom, Myhre et al., 2013). For this study, we have considered the following models: (i) the global aerosol-climate model ECHAM6-HAM (European Center for Medium-range Weather Forecasting model, Hamburg version, Zhang et al., 2012), (ii) GISS-modelE (ModelE version of the Goddard Institute for Space Studies, Koch et al., 2011), (iii) GFDL (Geophysical Fluid Dynamics Laboratory, Golaz et al., 2011), (iv) HadGEM3 (Hadley Center Global Environmental Model with the United Kingdom Chemistry and Aerosols, Bellouin et al., 2011), and (v) two versions of SPRINTARS (Spectral Radiation Transport Model for Aerosol Species, Takemura et al., 2009) models. The above models are driven by Aero-

Com emissions for the years 1850 and 2000 (Myhre et al., 2013). A detailed description of nudging and other model treatments is illustrated in Ghan et al. (2016). To study the aerosol-cloud interaction, we have used the GCMs with AeroCom emissions for the year 2000 with three hourly outputs. The aerosol-cloud sensitivity analysis is restricted to the marine stratocumulus clouds over the SEP during the VOCALS intensive experiment from 15 October 2008 to 15 November 2008. Further, the statistical method to calculate radiative forcing is only applied to the AeroCom GCMs. Because the statistical method uses the mean/median change in the LWP over the marine stratocumulus over SEP, that can be estimated only from the simulations with and without aerosol perturbation. Hence, we have used present-day and pre-industrial AeroCom solutions to calculate the change in LWP due to aerosol perturbation. A list of models used in this study, along with their resolutions, is given in Table 1.

2.3 Satellite observation

We have also used data from the Moderate Resolution Imaging Spectroradiometer (MODIS, Platnick et al., 2017) onboard the Aqua satellite. The MODIS satellite delivers daily information on the average cloud and aerosol properties within a 1° × 1° degree resolution (MODIS Level-3 product), with near-global coverage. The primary quantities of interest when investigating aerosol-cloud interaction are aerosol optical depth (AOD) and cloud effective radius (r_e), together with total liquid water path (LWP) and optical depth (τ_c) of the cloud. Although CDNC is not retrieved directly, it can be estimated using τ_c and r_e that uses the adiabatic assumption (Quaas et al., 2006), is given by; CDNC = $\alpha\, \tau_c^{0.5}\, r_e^{-2.5}$, where $\alpha = 1.37 \times 10^{-5}\, m^{-0.5}$. The CDNC is then filtered for single-layer liquid clouds with a cloud-top temperature greater than 268 K and pixels with a cloud fraction greater than 0.9. Additionally, a cloud optical depth of less than two is excluded from the analysis (Gryspeerdt et al., 2019). The CDNC is a crucial parameter for aerosol-cloud interaction because it influences cloud albedo by directly linking with aerosol sources (Wood et al., 2011). The uncertainties in the derived CDNC arise mainly from the cloud droplet effective radius (Grosvenor et al., 2018; Quaas et al., 2006). Further, they suggested that in the broken cloud regime and at the low zenith angle, the uncertainties are higher in the satellite retrieval of CDNC.

Table 1: *Details of models used in this study:*

No.	Models	Type	Model Resolutions
1.	WRF-Chem	Regional	0.25° × 0.25°
2.	COSMO-ART	Regional	0.01° × 0.05°
3.	ECHAM-HAM	GCM	2.50° × 2.5°
4.	HadGEM3	GCM	1.25° × 1.875°
5.	GFDL	GCM	2.50° × 2.5°
6.	GISS	GCM	2.50° × 2.5°
7.	SPRINTARS	GCM	2.50° × 2.5°

In both regional and GCMs, the top cloud CDNC is considered, and the analysis was restricted to liquid phase clouds. The sensitivity cloud microphysics on aerosol perturbation is studied using the joint histograms analysed following Gryspeerdt et al. (2016). In the joint histogram, for instance, the conditional probability is defined as the probability of finding a certain LWP given that a certain CDNC has been observed (CP = [P (LWP | CDNC) × 100]).

2.4 Radiative forcing

Atmospheric aerosols play an important role in modifying the Earth's radiation budget (Menon et al., 2002; Forster et al., 2007). An aerosol perturbation which alters the radiative balance at the top of the atmosphere (TOA) is aerosol radiative forcing. It results in a negative forcing (cooling) at TOA that partly offsets greenhouse warming. The global mean net radiative forcing estimate at TOA is -0.5 Wm^{-2} with an uncertainty of a factor of 2 (Forster et al., 2007). In the global model TOA, radiative forcing is defined as the difference between the radiative fluxes in the absence (pristine pre-industrial) and the presence of aerosol (present-day) (Loeb and Manalo-Smith, 2005). This radiative flux perturbation is a valid option for studying the forcing in different models (Lohmann et al., 2010). In this study, we have used AeroCom models (detailed description in section 2.2) with a baseline state of the atmosphere under pre-industrial conditions and the present state of the atmosphere under present-day conditions (Myhre et al., 2013). From these simulations, aerosol radiative forcing can be expressed as,

$$\Delta F_f = (F_{net}^{\downarrow} - F_{net}^{\uparrow})_{PD} - (F_{net}^{\downarrow} - F_{net}^{\uparrow})_{PI}$$
where, F_{net} = Shortwave + Longwave, PD = Present day, and PI = Pre-industrial (1)

Similarly, from the pre-industrial and present-day model simulation, one can also estimate the net radiative forcing at TOA using cloud optical properties. For this, one can use a joint histogram of CDNC (N_d) and LWP (L), one can choose most likely LWP corresponding to mean/median CDNC (N_d) for present-day and pre-industrial scenarios, the difference between the two LWP (L) is Δ L. With present-day τ_c, N_d, Δ L and assuming one of the g (asymmetry parameter)values (for example, g = 0.85), one can calculate the change in planetary albedo $\Delta\alpha$

$$\Delta\alpha = \frac{5}{6}\frac{(1-g)(a_2-a_1)}{(\tau_c(1-g)+a_2)^2}\frac{\tau_c}{L}\Delta L$$

Where a_1 and a_2 are constants, the corresponding values are 0.092, 1.43 respectively . Along with the TOA, incoming solar radiation $F_s^{\downarrow}$ and fractional coverage with liquid clouds f_{liq} yields TOA radiative forcing and can be expressed as (Quaas et al., 2008),

$$\Delta F_c = -f_{liq}F_s^{\downarrow}\Delta\alpha \quad (2)$$

In this study, the radiative forcing is representative of the months October and November, the intensive VOCALS experiment period and the forcing estimates are restricted to GCMs.

3 Results

3.1 Satellite climatology: aerosol optical depth and cloud optical properties

The monthly climatology of MODIS aqua-derived aerosol and cloud optical properties over SEP has been analyzed for the period of 15 October to 15 November 2004 - 2014. Fig. 1 shows the climatology of the spatial distribution of AOD, cloud fraction (CF), LWP,

and CDNC, respectively. The figure shows that the SEP is a region of low AOD, and it varies between 0.05 to 0.6 (Fig. 1 a). The relatively high AOD can be noticed over the land and adjoining areas. The increased aerosol loading over the land and the adjacent regions is due to the transport of polluted air mass from continental sources (Twohy et al., 2013). The climatological pattern of AOD indicates that SEP is a relatively clean area. The CF climatology suggests that over the oceanic region, the CF exceeds 50% (0.5), and reaches as high as 90% in most parts (Fig. 1 b). Muhlbauer et al. (2014) reported that marine stratocumulus exhibits different morphologies of cellular mesoscale convection, in which the CF is largest for closed mesoscale cellular convection with a mean of about 90% on a global scale. Fig. 1 c shows the LWP climatology with a significant increase over the land relative to the marine environment. The offshore LWP values exceed 250 gm^{-2}, with high values seen over the northwest region, whereas, over the maritime atmosphere, the LWP is observed below 100 gm^{-2}. Aircraft observation during the VOCALS experiment also reported a similar LWP pattern over SEP (Wyant et al., 2015). Further, the CDNC climatology, which is derived from MODIS cloud effective radius (r_e) and cloud optical depth (τ_c), also demonstrates an increase as it moves towards the coast. The offshore low CDNC indicates the existence of broad marine stratocumulus. Over the open ocean, the CDNC values are below 140 cm^{-3}, whereas in the coastal region, it ranges between 200 to 400 cm^{-3}. The climatological values are also in close agreement with VOCALS observation, in which the average CDNC ranges between 80 and 400 cm^{-3} (Zheng et al., 2011).

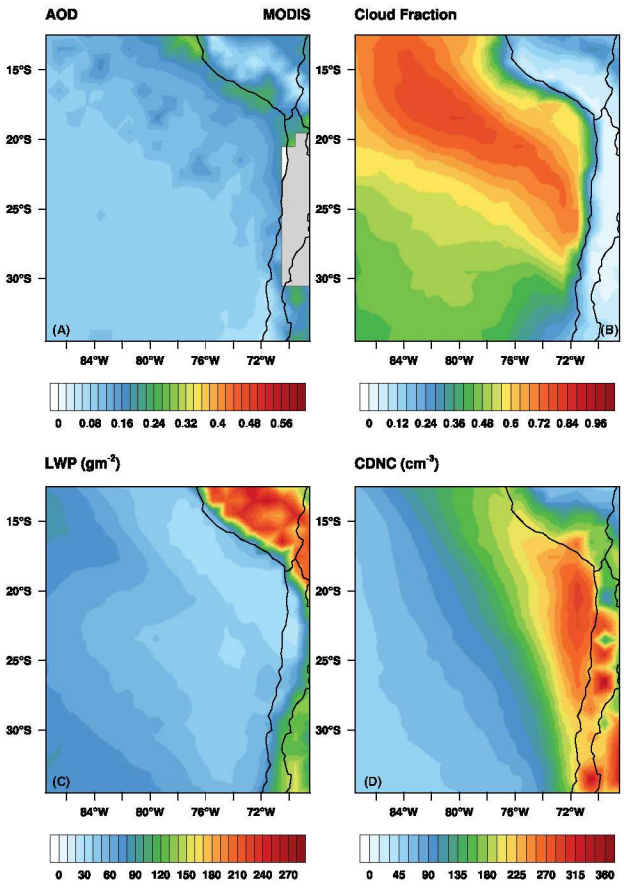

Figure 1: *MODIS climatology (2001-2014) of (a) aeroosl optical depth (AOD), (b) cloud fraction (CF, %), (c) liquid water path (LWP, g m^{-2}), and (d) cloud droplet number concentration (CDNC, c m^{-3}) over the SEP.*

3.2 Aerosol cloud interaction

3.2.1 Satellite analysis

The sensitivity of CDNC to AOD/LWP is investigated using the joint histogram analysis described by (Gryspeerdt et al., 2016). It relies on conditional probability, and the joint

histograms are normalized such that each column adds to unity. Fig. 2 shows the relation between AOD/CDNC-CDNC/LWP derived from the satellite observation over the SEP. Both monthly and climatological AOD-CDNC show a nonlinear relationship. For low AOD, the sensitivity to CDC is negative, with maximum condition probability seen along the negative slope. Then the AOD increases with increasing CDNC (Fig. 1 a and b), with maximum condition probability observed along the positive slope. The strong CDNC-AOD sensitivity at higher AOD is in agreement with previous studies (Quaas et al., 2008; Gryspeerdt et al., 2016). The nonlinearity in AOD-CDNC relation may arise from the poor retrieval of MODIS AOD below 0.05 along with CDNC retrieval uncertainty. Hence care must be taken in interpreting the AOD-CDNC relation (Gryspeerdt et al., 2016). Even though the AOD-CDNC relationship is nonlinear, the dominant relation is positive, especially for the AOD between 0.5 to 1.

In the case of CDNC-LWP relation, both the monthly and the climatology also show a similar pattern (Fig. 2 c and d). In both cases, the relationship is nonlinear, with a slight increase in LWP for the lower CDNC (< 20 cm^{-3}), then decreases with the increasing CDNC. Further, the maximum conditional probability is observed along the nonlinearity curve of the CDNC-LWP relation. Gryspeerdt et al. (2019) also reported a similar nonlinear CDNC-LWP sensitivity over the Global Oceans using satellite data. Although the joint histogram analysis shows a nonlinear relationship, the dominant tendency in both cases is a negative sensitivity.

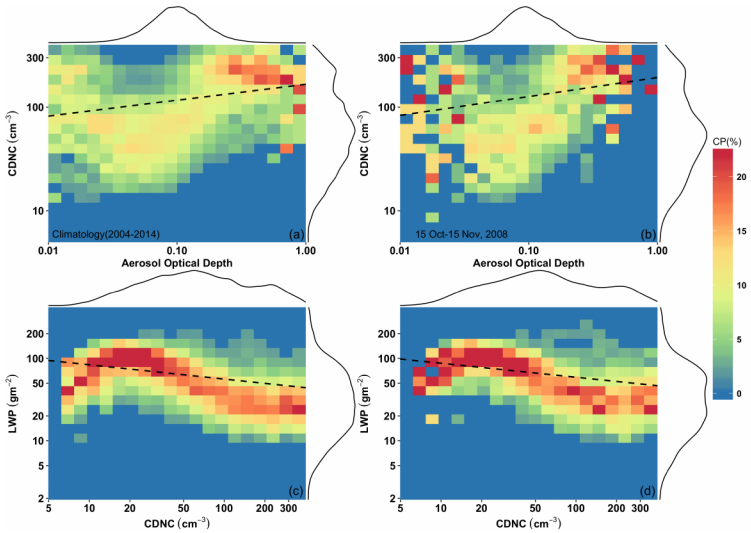

Figure 2: *The MODIS satellite-derived joint histogram for AOD-CDNC (a), climatology for the period 2004 to 2014, (b) monthly time scale (15 October to 15 November 2008), and the joint histogram for CDNC-LWP (c) climatology for the period 2004 to 2014, (d) monthly time scale (15 October to 15 November 2008). The dotted line in each plot represents the linear regression. CP(%) is condition probability: the probability of finding a certain CDNC(LWP) given that a certain AOD(CDNC) has been observed. The marginal plots are the probability density function (PDF) for the respective variables.*

3.2.2 Model analysis

Fig. 3 illustrates the AOD-CDNC sensitivity in the regional and global models. Both WRchem model shows a strong positive AOD-CDNC relationship (the maximum condition probability lies along the positive slope), while the COSMO-ART shows a weak AOD-CDNC sensitivity (Fig. 3 a, b, and c). As the aerosol increases, the CDNC also increases, which suggests a strong cloud lifetime effect in the WRF-chem model. In the case of COSMO-ART, the AOD-CDNC sensitivity is very weak because of the distribution of

AOD and CDNC in the model. In the COSMO-ART, the AOD values range between 0.01 and 0.2, whereas in the WRF, it ranges between 0.02 to 0.8. While the COSMO-ART simulated CDNC ranges between 5 to 300 cm^{-3} with a PDF (probability density function) the peak centred at 60 cm^{-3}. Although the WRF-Chem CDNC also shows similar distribution to that of the COSMO model, it is broader in the WRF-chem models. The GCMs, also show a diverse AOD-CDNC sensitivity, with most models showing a

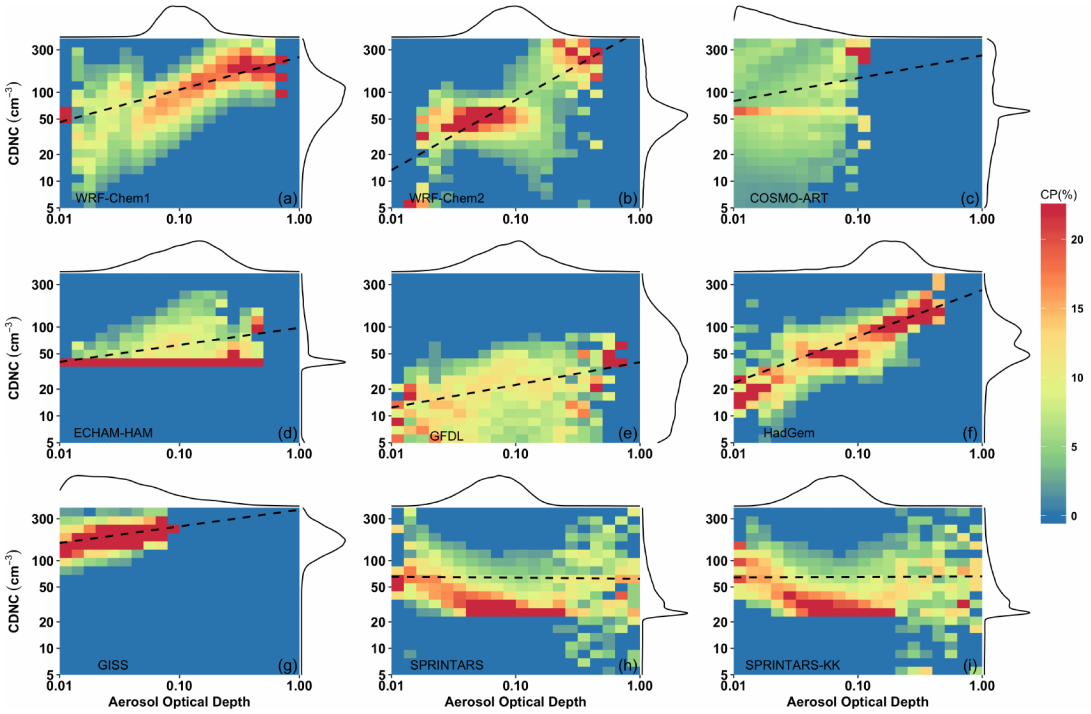

Figure 3: *The AOD-CDNC joint histogram for (a) WRF-Chem (IOWA), (b) WRF-Chem (PNNL), (c) COSMO-ART, (d) ECHAM-HAM, (e) GFDL, (f) HadGem, (g) GISS, (h) SPRINTARS, and (k) SPRINTARS-KK. The figure description is the same as Fig. 1.*

positive AOD-CDNC relation. In the case of ECHAM-HAM (Fig. 3 d), the maximum CP is lining along constant CDNC (50 cm^{-3}) because the lower limit of the prescribed CDNC is 40 cm^{-3}, although the rest of the plot shows a positive sensitivity. The models such as GFDL, HdGem, and GISS show a relatively strong positive AOD-CDNC sensitivity, with maximum CP appearing along the positive slope (Fig. 3 e, f, and g). At the same time, the SPRINTARS models show a weak AOD-CDNC sensitivity. Both SPRINTARS shows negative AOD-CDNC relation for the lower AODs, with maximum CP appearing along the negative slope. For higher AODs, the histograms are randomly distributed (Fig. 3 h and i).

The CDNC-LWP relationship from the regional and global model over the SEP is illustrated in Fig. 4. Both WRF-chem simulations show a strong negative CDNC-LWP relationship (Fig. 4 a and b), with maximum CP appearing along the negative slope. However, the COSMO-ART shows a strong positive relationship, with peak CP appearing along the positive slope (Fig.4 c). Again, the distinct CDNC-LWP relationship within the regional model arises due to the treatment of the microphysical processes in the models. Although the LWP distribution is similar in the regional models, the CDNC distribution in the COSMO-ART model is narrow compared to the WRF-chem.

Furthermore, the CDNC-LWP relationship in the global model also shows a diverse

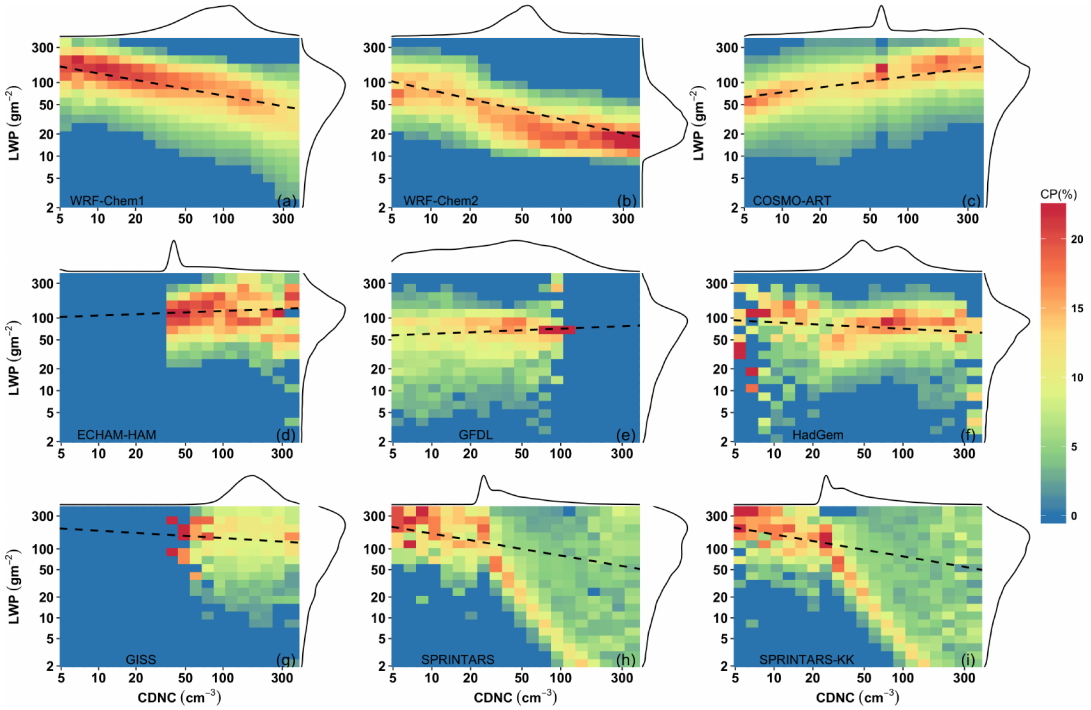

Figure 4: *The CDNC-LWP joint histogram for (a) WRF-Chem (IOWA), (b) WRF-Chem (PNNL), (c) COSMO-ART, (d) ECHAM-HAM, (e) GFDL, (f) HadGem, (g) GISS, (h) SPRINTARS, and (k) SPRINTARS-KK. The figure description is the same as Fig. 1.*

relationship. The ECHAM-HAM and the GFDL models show a somewhat positive relationship (Fig. 4 d and e). In contrast, a negative CDNC-LWP relationship dominates in the models HadGem, GISS and the SPRINTARS, respectively (Fig. 4, f, g, and h). Similar to the regional models, the diverse CDN-LWP relationship also arises due to the CDNC distribution in the respective models. In ECHAM-HAM and SPRINTARS, the CDNC distribution is narrow compared to other GCMs. However, all the GCMs show similar LWP distribution.

3.3 Radiative forcing estimates

The anthropogenic aerosol radiative forcing is estimated using two different methods. The first method uses the top of the atmosphere (TOA) flux between pre-industrial and present-day simulations (equation 1). The second method uses statistical relation using planetary albedo and cloud properties (equation 2). In this study, the radiative forcing estimates are restricted to the GCMs only (AeroCom models), focusing on the VOCALS region and experiment period. The GCM estimated aerosol radiative forcing is provided in Table 2. Even though the aerosol effect and the cloud microphysics are parameterized differently in the GCMs, in the flux method, all the GCMs are able to produce a net negative radiative forcing at the TOA (net cooling) similar to the global average. The multi-model flux-derived radiative forcing ranges from -1.03 to -3.58 W m^{-2}. The wide ranges of GCM radiative forcing are also reported in the previous studies (Quaas et al., 2009).

Table 2: *The net (Shortwave + Longwave) radiative forcing at the TOA over SEP:*

No	Models	ΔF_c at TOA ($W m^2$)		AOD		CDNC ($c m^{-3}$)		LWP ($g m^{-2}$)	
		Flux method	Statistical method	PD	PI	PD	PI	PD	PI
1	ECHAM-HAM	-1.64	-0.47	0.074	0.067	67	55	102.10	107.52
2	GFDL	-1.25	-3.29	0.076	0.058	22	11	61.84	46.77
3	HadGEM3	-3.58	0.78	0.098	0.072	73	56	75.11	72.16
4	GISS	-1.59	0.49	0.062	0.054	177	138	133.10	192.84
5	SPRINTARS	-1.03	1.05	0.071	0.063	50	47	111.80	111.71
6	SPRINTARS*	-1.08	1.08	0.066	0.058	51	47	96.39	95.23

R.F.: Radiative Forcing;
PD: Present Day
PI: Pre-Industrial
SPRINTARS*: SPRINTARS-KK

However, the negative radiative forcing didn't show any signs of the aerosol-cloud interaction (diverse CDNC-LWP sensitivity in GCMs); the statistical method could circumvent it. Similar to the diverse CDNC-LWP relation, the radiative forcing estimated using the statistical method shows different forcing in the GCMs. The ECHAM-HAM and GFDL models show similar radiative forcing (negative) in the statistical and the flux method. In the flux method, the estimated radiative forcings are -0.47 and -3.29 $W m^{-2}$, respectively, for the ECHAM-HAM and GFDL. The rest of the models depict positive radiative forcing of 0.776, 0.495, 1.051, and 1.08 $W m^{-2}$, respectively, for the models HadGEM3, GISS, and SPRINTARS. The CDNC-LWP joint histogram analysis shows a positive CDNC-LWP sensitivity in ECHAM-HAM and GFDL models. It implies that, as the CDNC increases, the LWP also increases, which leads to a negative radiative forcing. However, the rest of the GCMs are susceptible to a negative CDNC-LWP sensitivity, resulting in the positive radiative forcing. The statistical approach accounts for the effect of aerosol on the cloud's microphysical properties in the climate models, resulting in the diverse magnitude of the radiative forcing. Further, it can be due to the cloud microphysics (marine stratocumulus) parameterization in respective GCMs. The global liquid cloud fraction climatology from the GCMs shows large spatial and inter-model variability. Besides the SPRINTERS models, SEP marine stratocumulus clouds are represented quite well in the models, with varying magnitudes, though. Additionally the cloud representation in the GCMs, the factor contributing to the statistical radiative forcing is the sign of the ΔL (change in LWP, $\Delta L = \overline{L_{pd}} - \overline{L_{pi}}$). Thus, it is noticed that in the ECHAM-HAM and GFDL models, marine stratocumulus clouds are more susceptible to aerosols ($-\Delta L$), resulting in a negative radiative forcing. However, in other GCMs, the marine stratocumulus clouds are not susceptible to aerosol perturbation ($+\Delta L$), resulting in a positive radiative forcing.

4 Summary and conclusions

The aerosol-cloud interaction in the marine stratocumulus cloud over the SEP has been invested using satellite observation and multi-model simulations. The MODIS climatology of AOD indicates that SEP is a region of relatively low aerosol loading. The SEP coastal and adjoining regions are relatively polluted compared to the maritime atmo-

sphere. Over the SEP, the MODIS AOD varies between 0.1 to 0.6. The CF climatology shows there is a persistent cloud cover over the ocean, which attributes to the marine stratocumulus deck over the SEP. The annual mean CF exceeds 60% in most regions, except over the coast, where topographic irregularities exist. The corresponding LWP is dominant over the coastal region, which varies between 30 to 300 $\mathrm{g\,m^{-3}}$. Additionally, the CDNC climatology shows a latitudinal gradient with maximum CDNC observed in the coastal region. It is consistent with previous studies (Wyant et al., 2015).

To explore the cloud susceptibility to aerosol loading, we have used a joint histogram of AOD-CDNC and CDNC-LWP. The MODIS satellite analysis shows that on both monthly and climatological time scales, the AOD-CDNC relation shows a dominant positive relation, despite the non-linearity at lower AOD. In contrast, the CDNC-LWP shows a negative sensitivity. A positive AOD-CDNC suggests the cloud albedo effect in the marine stratocumulus clouds (Twomey, 1977; Albrecht, 1989). However, the CDNC-LWP relation shows that the cloud albedo effect (a positive CDNC-LWP relation) is observed only at lower CDNC. The CDNC-LWP relation is dominant, with a negative CDNC-LWP sensitivity that accounts for the cloud droplet entrainment and evaporation (Han et al., 2002).

Further, we have explored aerosol-cloud interaction over the SEP using regional and climate model simulations. The joint histogram analysis shows that both WRF-chem models show a relatively strong AOD-CDNC relation in the regional model compared to the COSMO-ART model. The weak AOD-CDNC relationship in the COSMO-ART model may be due to the poor representation of aerosols in the model compared to WRF-chem. The PDF shows that the AOD distribution is skewed to the right in the COSMO-ART. However, the CDNC shows the normal distribution in the COSMO-ART, which is comparable with WRF-chem. Furthermore, besides the SPRINTERS model, the GCMs also show a positive AOD-CDNC sensitivity over the SEP region. In the case of the CDNC-LWP sensitivity, both the WRF-chem models show a strong negative relationship. At the same time, in the COSMO-ART, the CDNC-LWP shows a strong positive relationship. Likewise, the Aerocom models also depict a diverse CDNC-LWP relationship. In ECHAM-HAM and the GFDL model, a positive CDNC-LWP relation is observed, whereas a negative CDNC-LWP relation is seen in HadGEM, GISS, and SPRINTARS models, respectively.

From the satellite analysis, it is noticed that the AOD-CDNC relation mainly accounts for the cloud lifetime or cloud albedo effect. However, the non-linear CDNC-LWP relation suggests both cloud albedo and entrainment effects. In the case of AOD-CDNC sensitivity derived from the models, most of the model represents the cloud albedo effect. It suggests that, as the aerosol concentration increases, the CDNC also increases, leading to the cloud albedo effect, consequently, a negative radiative forcing. Notably, all the GCMs reveal a negative radiative forcing at the TOA while using the flux method, which is similar to the global mean radiative forcing. However, the radiative forcings are diverse when we use the statistical method, which would also consider the effect of LWP sensitivity to aerosol perturbation. The above analysis suggests that the flux-derived radiative forcing results in net cooling at the TOA irrespective of the model, even though aerosol and cloud parameterizations are treated differently. Further, the GCM models are tuned radiatively to get similar radiative forcing at the TOA. So our analysis suggests that the statistical approach using planetary albedo and cloud properties would be more

appropriate for radiative forcing estimates in which aerosol-mediated indirect effects are also considered. Importantly, the statistical method assumes that the CDNC-LWP sensitivity is linear and the LWP is susceptible to aerosol loading. However, recent studies (in addition to this analysis) suggest that the CDNC-LWP relation is non-linear (Gryspeerdt et al., 2019). So further research would be needed to improve the statistical method to predict the radiative forcing.

Acknowledgements

This study has been carried out as a part of the Aerosols, Clouds, Precipitation and Climate (ACPC) initiative. We thank the VOCALS and KIT group for providing the regional model simulations.

References

Albrecht, B. A.: Aerosols, Cloud Microphysics, and Fractional Cloudiness, Science, 245, 1227–1230, doi:10.1126/science.245.4923.1227, URL http://science.sciencemag.org/content/245/4923/1227, 1989.

Bellouin, N., Rae, J., Jones, A., et al.: Aerosol forcing in the Climate Model Intercomparison Project (CMIP5) simulations by HadGEM2-ES and the role of ammonium nitrate, Journal of Geophysical Research: Atmospheres, 116, n/a–n/a, doi:10.1029/2011JD016074, URL http://dx.doi.org/10.1029/2011JD016074, d20206, 2011.

Bellouin, N., Quaas, J., Gryspeerdt, E., et al.: Bounding global aerosol radiative forcing of climate change, Rev. Geophys., 58, e2019RG000 660, doi:10.1029/2019RG000660, 2020.

Charlson, R. J., Schwartz, S. E., Hales, J. M., et al.: Climate Forcing by Anthropogenic Aerosols, Science, 255, 423–430, doi:10.1126/science.255.5043.423, URL https://science.sciencemag.org/content/255/5043/423, 1992.

Forster, P., Ramaswamy, V., Artaxo, P., et al.: Changes in Atmospheric Constituents and in Radiative Forcing, pp. 129–234, Cambridge University Press, Cambridge, United Kingdom and New York, NY, USA, 2007.

Forster, P., Storelvmo, T., Armour, K., et al.: The Earth's Energy Budget, Climate Feedbacks, and Climate Sensitivity. In *Climate Change 2021: The Physical Science Basis. Contribution of Working Group I to the Sixth Assessment Report of the Intergovernmental Panel on Climate Change* [Masson-Delmotte, V., P. Zhai, A. Pirani, S.L. Connors, C. Péan, S. Berger, N. Caud, Y. Chen, L. Goldfarb, M.I. Gomis, M. Huang, K. Leitzell, E. Lonnoy, J.B.R. Matthews, T.K. Maycock, T. Waterfield, O. Yelekçi, R. Yu, and B. Zhou (eds)], chap. 7, Cambridge University Press. In Press., 2021.

Ghan, S., Wang, M., Zhang, S., et al.: Challenges in constraining anthropogenic aerosol effects on cloud radiative forcing using present-day spatiotemporal variability, Proceedings of the National Academy of Sciences, 113, 5804–5811, doi:10.1073/pnas.1514036113, URL http://www.pnas.org/content/113/21/5804.abstract, 2016.

Golaz, J.-C., Salzmann, M., Donner, L. J., et al.: Sensitivity of the Aerosol Indirect Effect to Subgrid Variability in the Cloud Parameterization of the GFDL Atmosphere General Circulation Model AM3, Journal of Climate, 24, 3145–3160, doi:10.1175/2010JCLI3945.1, URL https://doi.org/10.1175/2010JCLI3945.1, 2011.

Goren, T. and Rosenfeld, D.: Satellite observations of ship emission induced transitions from broken to closed cell marine stratocumulus over large areas, Journal of Geophysical Research: Atmospheres, 117, n/a–n/a, doi:10.1029/2012JD017981, URL http://dx.doi.org/10.1029/2012JD017981, d17206, 2012.

Goren, T. and Rosenfeld, D.: Extensive closed cell marine stratocumulus downwind of Europe—A large aerosol cloud mediated radiative effect or forcing?, Journal of Geophysical Research: Atmospheres, 120, 6098–6116, doi:10.1002/2015JD023176, URL http://dx.doi.org/10.1002/2015JD023176, 2015JD023176, 2015.

Grell, G. A., Peckham, S. E., Schmitz, R., et al.: Fully coupled "online" chemistry within the WRF model, Atmospheric Environment, 39, 6957–6975, doi:https://doi.org/10.1016/j.atmosenv.2005.04.027, URL https://www.sciencedirect.com/science/article/pii/S1352231005003560, 2005.

Grosvenor, D. P., Sourdeval, O., Zuidema, P., et al.: Remote Sensing of Droplet Number Concentration in Warm Clouds: A Review of the Current State of Knowledge and Perspectives, Reviews of Geophysics, 56, 409–453, doi:https://doi.org/10.1029/2017RG000593, URL https://agupubs.onlinelibrary.wiley.com/doi/abs/10.1029/2017RG000593, 2018.

Gryspeerdt, E., Quaas, J., and Bellouin, N.: Constraining the aerosol influence on cloud fraction, Journal of Geophysical Research: Atmospheres, 121, 3566–3583, doi:10.1002/2015JD023744, URL http://dx.doi.org/10.1002/2015JD023744, 2015JD023744, 2016.

Gryspeerdt, E., Goren, T., Sourdeval, O., et al.: Constraining the aerosol influence on cloud liquid water path, Atmos. Chem. Phys., 19, 5331–5347, doi:10.5194/acp-19-5331-2019, URL https://acp.copernicus.org/articles/19/5331/2019/, 2019.

Han, Q., Rossow, W. B., Zeng, J., and Welch, R.: Three Different Behaviors of Liquid Water Path of Water Clouds in Aerosol–Cloud Interactions, Journal of the Atmospheric Sciences, 59, 726–735, doi:10.1175/1520-0469(2002)059<0726:TDBOLW>2.0.CO;2, URL https://doi.org/10.1175/1520-0469(2002)059<0726:TDBOLW>2.0.CO;2, 2002.

Koch, D., Bauer, S. E., Genio, A. D., et al.: Coupled Aerosol-Chemistry–Climate Twentieth-Century Transient Model Investigation: Trends in Short-Lived Species and Climate Responses, Journal of Climate, 24, 2693–2714, doi:10.1175/2011JCLI3582.1, URL https://doi.org/10.1175/2011JCLI3582.1, 2011.

Loeb, N. G. and Manalo-Smith, N.: Top-of-Atmosphere Direct Radiative Effect of Aerosols over Global Oceans from Merged CERES and MODIS Observations, Journal of Climate, 18, 3506–3526, doi:10.1175/JCLI3504.1, URL https://doi.org/10.1175/JCLI3504.1, 2005.

Lohmann, U., Rotstayn, L., Storelvmo, T., et al.: Total aerosol effect: radiative forcing or radiative flux perturbation?, Atmospheric Chemistry and Physics, 10, 3235–3246, doi:10.5194/acp-10-3235-2010, URL https://www.atmos-chem-phys.net/10/3235/2010/, 2010.

McComiskey, A. and Feingold, G.: The scale problem in quantifying aerosol indirect effects, Atmospheric Chemistry and Physics, 12, 1031–1049, doi:10.5194/acp-12-1031-2012, URL https://www.atmos-chem-phys.net/12/1031/2012/, 2012.

Menon, S., Genio, A. D. D., Koch, D., and Tselioudis, G.: GCM Simulations of the Aerosol Indirect Effect: Sensitivity to Cloud Parameterization and Aerosol Burden, Journal of the Atmospheric Sciences, 59, 692–713, doi:10.1175/1520-0469(2002)059<0692:GSOTAI>2.0.CO;2, URL https://doi.org/10.1175/1520-0469(2002)059<0692:GSOTAI>2.0.CO;2, 2002.

Menon, S., Genio, A. D., Kaufman, Y., et al.: Analyzing signatures of aerosol-cloud interactions from satellite retrievals and the GISS GCM to constrain the aerosol indirect effect, Journal of Geophysical Research, 113, 1–15, doi:10.1029/2007JD009442, 2008.

Min, Q., Joseph, E., Lin, Y., et al.: Comparison of MODIS cloud microphysical properties with in-situ measurements over the Southeast Pacific, Atmospheric Chemistry and Physics, 12, 11 261–11 273, doi:10.5194/acp-12-11261-2012, URL https://www.atmos-chem-phys.net/12/11261/2012/, 2012.

Muhlbauer, A., McCoy, I. L., and Wood, R.: Climatology of stratocumulus cloud morphologies: microphysical properties and radiative effects, Atmospheric Chemistry and Physics, 14, 6695–6716, doi:10.5194/acp-14-6695-2014, URL https://www.atmos-chem-phys.net/14/6695/2014/, 2014.

Mülmenstädt, J. and Feingold, G.: The Radiative Forcing of Aerosol-Cloud Interactions in Liquid Clouds: Wrestling and Embracing Uncertainty, Curr. Clim. Chang. Rep., 4, 23–40, doi:10.1007/s40641-018-0089-y, URL https://doi.org/10.1007/s40641-018-0089-y, 2018.

Myhre, G., Samset, B. H., Schulz, M., et al.: Radiative forcing of the direct aerosol effect from AeroCom Phase II simulations, Atmospheric Chemistry and Physics, 13, 1853–1877, doi:10.5194/acp-13-1853-2013, URL https://www.atmos-chem-phys.net/13/1853/2013/, 2013.

Platnick, S., Meyer, K. G., King, M. D., et al.: The MODIS Cloud Optical and Microphysical Products: Collection 6 Updates and Examples From Terra and Aqua, IEEE Trans. Geosci. Remote Sens., 55, 502–525, doi:10.1109/TGRS.2016.2610522, 2017.

Quaas, J., Boucher, O., and Lohmann, U.: Constraining the total aerosol indirect effect in the LMDZ and ECHAM4 GCMs using MODIS satellite data, Atmospheric Chemistry and Physics, 6, 947–955, doi:10.5194/acp-6-947-2006, URL https://www.atmos-chem-phys.net/6/947/2006/, 2006.

Quaas, J., Boucher, O., Bellouin, N., and Kinne, S.: Satellite-based estimate of the direct and indirect aerosol climate forcing, Journal of Geophysical Research: Atmospheres, 113, n/a–n/a, doi:10.1029/2007JD008962, URL http://dx.doi.org/10.1029/2007JD008962, d05204, 2008.

Quaas, J., Ming, Y., Menon, S., et al.: Aerosol indirect effects â€“ general circulation model intercomparison and evaluation with satellite data, Atmospheric Chemistry and Physics, 9, 8697–8717, doi:10.5194/acp-9-8697-2009, URL https://www.atmos-chem-phys.net/9/8697/2009/, 2009.

Saide, P. E., Spak, S. N., Carmichael, G. R., et al.: Evaluating WRF-Chem aerosol indirect effects in Southeast Pacific marine stratocumulus during VOCALS-REx, Atmospheric Chemistry and Physics, 12, 3045–3064, doi:10.5194/acp-12-3045-2012, URL https://acp.copernicus.org/articles/12/3045/2012/, 2012.

Takemura, T., Egashira, M., Matsuzawa, K., et al.: A simulation of the global distribution and radiative forcing of soil dust aerosols at the Last Glacial Maximum, Atmospheric Chemistry and Physics, 9, 3061–3073, doi:10.5194/acp-9-3061-2009, URL https://www.atmos-chem-phys.net/9/3061/2009/, 2009.

Twohy, C. H., Anderson, J. R., Toohey, D. W., et al.: Impacts of aerosol particles on the microphysical and radiative properties of stratocumulus clouds over the southeast Pacific Ocean, Atmospheric Chemistry and Physics, 13, 2541–2562, doi:10.5194/acp-13-2541-2013, URL https://www.atmos-chem-phys.net/13/2541/2013/, 2013.

Twomey, S.: The Influence of Pollution on the Shortwave Albedo of Clouds, Journal of the Atmospheric Sciences, 34, 1149–1152, doi:10.1175/1520-0469(1977)034<1149:TIOPOT>2.0.CO;2, URL https://doi.org/10.1175/1520-0469(1977)034<1149:TIOPOT>2.0.CO;2, 1977.

Vogel, B., Hoose, C., Vogel, H., and Kottmeier, C.: A model of dust transport applied to the Dead Sea Area, Meteorologische Zeitschrift, 15, 611–624, doi:10.1127/0941-2948/2006/0168, URL http://dx.doi.org/10.1127/0941-2948/2006/0168, 2006.

Wang, H., Rasch, P. J., and Feingold, G.: Manipulating marine stratocumulus cloud amount and albedo: a process-modelling study of aerosol-cloud-precipitation interactions in response to injection of cloud condensation nuclei, Atmospheric Chemistry and Physics, 11, 4237–4249, doi:10.5194/acp-11-4237-2011, URL https://www.atmos-chem-phys.net/11/4237/2011/, 2011.

Wood, R., Mechoso, C. R., Bretherton, C. S., et al.: The VAMOS Ocean-Cloud-Atmosphere-Land Study Regional Experiment (VOCALS-REx): goals, platforms, and field operations, Atmospheric Chemistry and Physics, 11, 627–654, doi:10.5194/acp-11-627-2011, URL https://www.atmos-chem-phys.net/11/627/2011/, 2011.

Wyant, M. C., Bretherton, C. S., Wood, R., et al.: Global and regional modeling of clouds and aerosols in the marine boundary layer during VOCALS: the VOCA intercomparison, Atmospheric Chemistry and Physics, 15, 153–172, doi:10.5194/acp-15-153-2015, URL https://www.atmos-chem-phys.net/15/153/2015/, 2015.

Yang, Q., Gustafson Jr., W. I., Fast, J. D., et al.: Impact of natural and anthropogenic aerosols on stratocumulus and precipitation in the Southeast Pacific: a regional modelling study using WRF-Chem, Atmospheric Chemistry and Physics, 12, 8777–8796, doi:10.5194/acp-12-8777-2012, URL https://www.atmos-chem-phys.net/12/8777/2012/, 2012.

Zhang, K., O'Donnell, D., Kazil, J., et al.: The global aerosol-climate model ECHAM-HAM, version 2: sensitivity to improvements in process representations, Atmospheric Chemistry and Physics, 12, 8911–8949, doi:10.5194/acp-12-8911-2012, URL https://www.atmos-chem-phys.net/12/8911/2012/, 2012.

Zheng, X., Albrecht, B., Jonsson, H. H., et al.: Observations of the boundary layer, cloud, and aerosol variability in the southeast Pacific near-coastal marine stratocumulus during VOCALS-REx, Atmospheric Chemistry and Physics, 11, 9943–9959, doi:10.5194/acp-11-9943-2011, URL https://www.atmos-chem-phys.net/11/9943/2011/, 2011.